Estimating insulin sensitivity after exercise using an Unscented Kalman Filter ⋆

Julia Deichmann [*,**] **Hans-Michael Kaltenbach** [*]

[*] *Department of Biosystems Science and Engineering, ETH Zurich, Basel, Switzerland; SIB Swiss Institute for Bioinformatics, Switzerland. (e-mail: julia.deichmann@bsse.ethz.ch; michael.kaltenbach@bsse.ethz.ch)*
[**] *Life Science Zurich Graduate School, Zurich, Switzerland.*

Abstract: Insulin sensitivity is an important physiological parameter for determining insulin requirements for patients with type 1 diabetes. In addition to being highly variable between patients, insulin sensitivity increases substantially during exercise and stays elevated for several hours during subsequent recovery. We propose an unscented Kalman filter for estimating insulin sensitivity from continuous glucose monitoring data that does not require the underlying model to capture exercise and relies on average values for patient-specific parameters. Using in silico full-day simulations including exercise and meals, we study how adjusting insulin doses for elevated insulin sensitivity could decrease the risk of hypoglycemia after exercise and improve time-in-range and related metrics.

Keywords: diabetes management; clinical guidelines; decision support; biological and medical system modelling; quantification of physiological parameters; insulin sensitivity; exercise

1. INTRODUCTION

Glucose homeostasis is a fundamental physiological process in healthy individuals that maintains plasma glucose levels in a narrow range of 70–140 mg/dl despite disturbances such as meals or exercise. The two hormones glucagon and insulin, produced in pancreatic α- and β-cells, respectively, are the two main regulators to achieve glucose homeostasis by promoting glucose production respectively glucose uptake by muscles and the liver, where glucose is converted into glycogen. Type 1 diabetes (T1D) is a common endocrine disorder resulting from autoimmune destruction of pancreatic β-cells. Patients are unable to produce insulin to maintain glucose homeostasis, and require exogenous insulin to mimic the natural glucose-insulin regulation and avoid persistent elevated blood glucose (hyperglycemia) (American Diabetes Association, 2014). Basal insulin levels are provided either by continuous infusion of insulin (in continuous subcutaneous insulin infusion (CSII) therapy) or by typically two daily injections of long-acting insulin (in multiple daily injection (MDI) therapy) to maintain glucose homeostasis in fasting conditions. In addition, meals are compensated by bolus injections of rapid-acting insulin in both forms of therapy (Janež et al., 2020), where the required dose depends on the amount of carbohydrates (CHO) in the meal, the insulin on board (IOB) from previous injections, and the current deviation from the blood glucose target. Bolus calculations also consider the patient-specific baseline insulin sensitivity that describes the decrease in blood glucose per unit of insulin administered. This parameter is highly variable between patients and is determined clinically, e.g., by a glucose tolerance test (Bergman et al., 1979).

Moreover, insulin sensitivity increases temporarily during exercise, and remains elevated for several hours during recovery, requiring additional adjustment of the basal and bolus insulin treatment (Annan, 2016). While generic clinical guidelines exist, the accurate adjustment to exercise demands precise tailoring to the patient and situation, and presents a major challenge. In particular, exercise-induced hypoglycemia (low blood glucose) can occur acutely, but also several hours after the activity due to the prolonged elevation of insulin sensitivity, where hypoglycemia is associated with acute complications such as dizziness and unconsciousness. While advances in sensors now provide blood glucose levels almost in real-time with continuous glucose monitoring (CGM) devices, insulin sensitivity is not amenable to direct measurement and needs to be inferred from the glucose measurement.

Here, we consider the problem of adjusting basal and bolus insulin calculations for increased insulin sensitivity from exercise. We use an unscented Kalman filter (UKF) (Julier and Uhlmann, 1997) to estimate the insulin sensitivity from CGM measurements and use this estimate to propose a reduction of the insulin bolus for a post-exercise meal as well as for a reduction of overnight basal insulin to avoid hypoglycemia. Kalman filters have been previously used to estimate blood glucose (Knobbe and Buckingham, 2005) and plasma insulin concentration (Eberle and Ament, 2011; de Pereda et al., 2015), and to track changes in insulin sensitivity (Boiroux et al., 2017) from CGM measurements, but not for exercise-related insulin therapy adjustments.

⋆ This work was supported by the two Cantons of Basel through project grant PMB-01-17 granted by the ETH Zurich.

We use a T1D model with exercise at moderate intensity together with an established CGM model to generate full-day data for a virtual patient population. Importantly, our observer model for the UKF only contains those model parts unrelated to exercise, and the UKF can thus not use predictions of exercise effects for the state estimation. Moreover, the UKF model has to rely on average values for all parameters, including the patient-specific and highly variable baseline insulin sensitivity and meal absorption parameters that we randomly perturb for each meal in our simulations. As a proof-of-principle, we show that reducing insulin doses based on the estimated insulin sensitivity can lead to reduced hypoglycemia and improved time-in-range.

2. METHODS

Our goal is the estimation of a patient's insulin sensitivity $S_I(t)$ in the presence of disturbances such as exercise. We consider this problem as a state estimation problem and propose using an unscented Kalman filter that uses information on previous insulin injections (u and u_b), carbohydrate intake (D) and a noisy measurement of interstitial glucose $\tilde{G}_I$ from a CGM device. We then use the estimated insulin sensitivity to adjust calculations for bolus insulin doses u and basal insulin requirements u_b (Fig. 1).

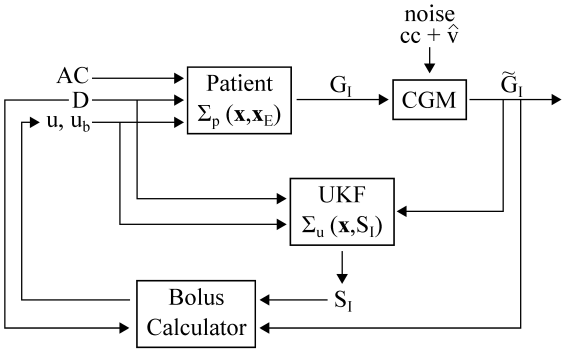

Fig. 1. Schematic of the UKF-assisted bolus calculator: A patient model Σ_p simulates interstitial glucose levels G_I considering exercise (AC), meals (D) and insulin (u, u_b). A CGM model generates noisy observations $\tilde{G}_I$ as input to an unscented Kalman filter with internal model Σ_u. The estimated insulin sensitivity S_I is used to adjust insulin requirements in a bolus calculator.

2.1 Observer Model

Our unscented Kalman filter uses an internal model for estimating the insulin sensitivity $S_I(t)$ that comprises: (i) a component to describe glucose-insulin dynamics derived from the two-compartment Minimal Model (Cobelli et al., 1999), (ii) a two-compartment component to describe the dynamics of plasma insulin following a subcutaneous injection of size u (Nucci and Cobelli, 2000), and (iii) a simple two-compartment component to describe changes in blood glucose following a meal of size D. We denote the model as Σ_u to distinguish it from the model used for simulating patient data (cf. Fig. 1).

The glucose-insulin dynamics (Cobelli et al., 1999) are given by

$$\begin{aligned}\dot{X}(t) &= S_I(t)\cdot p_2\cdot I(t) - p_2 X(t)\\ \dot{Q}_1(t) &= -[p_1+p_4]\cdot Q_1(t)\\ &\quad -X(t)\cdot Q_1(t)\\ &\quad +p_5\cdot Q_2(t) + EGP_0 + Ra(t)\\ \dot{Q}_2(t) &= p_4\cdot Q_1(t) - p_5\cdot Q_2(t)\\ \dot{S}_I(t) &= 0\\ G(t) &= Q_1(t)/V_g,\end{aligned} \tag{1}$$

where X [1/min] is remote insulin acting on plasma glucose, I [μU/ml] is plasma insulin concentration, Q_1 and Q_2 [mg/kg] are glucose masses in an accessible and non-accessible compartment, respectively, and G [mg/dl] is plasma glucose concentration. Insulin sensitivity is represented by state S_I [ml/μU/min] and modulates the action of plasma insulin I. The parameter EGP_0 [mg/kg/min] is the glucose production rate at zero glucose and Ra [mg/kg/min] is the glucose appearance rate from meals; p_1 to p_5 [1/min] are rate parameters, and V_g [dl/kg] is the glucose distribution volume. We stress that this model does not entail any processes—such as exercise—that would modify the insulin sensitivity $S_I(t)$ and the corresponding observer can therefore not rely on any predictions of such processes.

In this paper, we mainly consider MDI therapy. To describe the transfer of injected insulin from subcutaneous tissue into plasma, we introduce two compartments of subcutaneous insulin mass x_1 and x_2 [μU] and one plasma insulin compartment I [μU/ml] (Nucci and Cobelli, 2000):

$$\begin{aligned}\dot{x}_1(t) &= -k_1\cdot x_1(t) + u(t) + u_b\\ \dot{x}_2(t) &= k_1\cdot x_1(t) - (k_2+k_3)\cdot x_2(t)\\ \dot{I}(t) &= \frac{k_2}{V_i\cdot BW}\cdot x_2(t) - k_4\cdot I(t),\end{aligned} \tag{2}$$

where u [μU/min] is the rate of correction insulin injection, and u_b [μU/min] is the rate of basal insulin infusion, which we assume to be constant to mimic MDI therapy; k_1 to k_4 [1/min] are rate parameters, V_i [ml/kg] is the insulin distribution volume and BW [kg] is the patient's bodyweight.

To describe the glucose appearance rate Ra after carbohydrate ingestion, we consider the following two-compartment model:

$$\begin{aligned}\dot{M}_1(t) &= -m_1\cdot M_1(t) + D(t)\\ \dot{M}_1(t) &= m_1\cdot M_1(t) - m_2\cdot M_2(t)\\ Ra(t) &= \frac{f\cdot m_2}{BW}\cdot M_2(t),\end{aligned} \tag{3}$$

where D [mg/min] is the ingested glucose, m_1 and m_2 [1/min] are rate parameters and f specifies the fraction of glucose absorbed into plasma. This model is similar to the meal model proposed by Hovorka et al. (2004).

Continuous glucose monitoring does not measure the plasma glucose concentration G directly, but rather the corresponding interstitial glucose G_I [mg/dl], which leads to a time-delay between plasma glucose and measured glucose. We describe this transition using a model by Facchinetti et al. (2014) as

$$\dot{G}_I(t) = \frac{1}{\tau_G}(G(t) - G_I(t)), \tag{4}$$

with time constant $\tau_G = 6.7\,\text{min}$.

Parameter values are given in Table A.1. With $\mathbf{x} = (X, Q_1, Q_2, x_1, x_2, I, M_1, M_2, G_I)$, the state vector of Σ_u is $(\mathbf{x}, S_I)$.

2.2 Unscented Kalman Filter

We use an unscented Kalman filter for estimation of the state vector $(\mathbf{x}, S_I)$ based on the (discretized) observer model, glucose measurements of the state G_I and information on insulin injections (u and u_b) and meals (D). The UKF approach selects a set of points, called sigma points, spread around the mean of the current state estimate to propagate through the model and generate a new state estimate. We place the sigma points according to Julier and Uhlmann (1997) with $\kappa = 2$. Further, we initialize the diagonal covariance matrix P with the following uncertainties for the states $(\mathbf{x}, S_I)$: $\sigma = (1.65 \cdot 10^{-3}, 14.2, 9.3, 8511, 5833, 1.0, 10^{-3}, 10^{-3}, 11, 1.65 \cdot 10^{-4})$, amounting to around 10% of the initial state values. We define the diagonal elements of the process noise matrix Q according to $\sigma = (1.65 \cdot 10^{-4}, 1.42, 0.93, 851, 583, 0.1, 100, 50, 1.1, 1.65 \cdot 10^{-5})$, assuming a noise level of around 1% in each state. Finally, we assume a CGM measurement noise of $\sigma_{GI} = 15\text{mg/dl}$ for the 1×1 noise matrix R.

2.3 Simulation Model

To evaluate the performance of the state estimation and the subsequent bolus calculation, we generate blood glucose trajectories over a full day including three meals and an exercise session for a set of patients in silico. Our simulation model uses the same components as in Eq. 2 and Eq. 3 of the observer model for insulin injections and meals. We augment the glucose-insulin dynamics by several equations describing changes in glucose uptake and production during and after exercise, and consider the exercise-driven change in insulin sensitivity explicitly. Specifically, we describe the glucose-insulin dynamics as

$$\begin{aligned} \dot{X}(t) &= S_{I,0} \cdot p_2 \cdot I(t) - p_2 X(t) \\ \dot{Q}_1(t) &= -[p_1 + r_{GU} - r_{GP} + p_4] \cdot Q_1(t) \\ &\quad -(1 + Z(t)) \cdot X(t) \cdot Q_1(t) \\ &\quad +p_5 \cdot Q_2(t) + EGP_0 + Ra(t) \\ \dot{Q}_2(t) &= p_4 \cdot Q_1(t) - p_5 \cdot Q_2(t) \\ G(t) &= Q_1(t)/V_g, \end{aligned} \tag{5}$$

where $S_{I,0}$ is the (unperturbed) baseline insulin sensitivity of the patient, r_{GU}, r_{GP} and Z are exercise processes described below, and the remaining states and parameters are as in Eq. 1.

We capture exercise intensity Y by accelerometer counts AC [1/min] with delay τ_{AC} [min]:

$$\dot{Y}(t) = \frac{1}{\tau_{AC}}(AC(t) - Y(t)) \,. \tag{6}$$

Exercise triggers a range of processes, which we describe via increases in glucose uptake r_{GU} and production r_{GP} [1/min]:

$$\begin{aligned} \dot{r}_{GU}(t) &= q_1 \cdot f(Y) \cdot Y(t) - q_2 \cdot r_{GU}(t) \\ \dot{r}_{GP}(t) &= q_3 \cdot f(Y) \cdot Y(t) - q_4 \cdot r_{GP}(t), \end{aligned} \tag{7}$$

with rate parameters q_1 to q_4 [1/min] and a function $f(Y) = (Y/a)^n/[1 + (Y/a)^n]$ that provides the transition between rest and exercise. Moreover, insulin sensitivity increases by a factor $(1 + Z)$ due to exercise, where Z is given by

$$\dot{Z}(t) = b \cdot f(Y) \cdot Y(t) - \frac{1}{\tau_Z} \cdot (1 - f(Y)) \cdot Z(t) \,, \tag{8}$$

with parameter b and time constant τ_Z [min]. These extensions are comparable to exercise models presented by Breton (2008) and Roy and Parker (2007).

The resulting blood glucose G is translated into interstitial glucose G_I using Eq. 4, and we add two autoregressive noise processes to emulate measurement noise and generate the simulated measured glucose concentrations $\tilde{G}_I$ as input into the state estimator:

$$\tilde{G}_I(t) = G_I(t) + cc(t) + \hat{v}(t), \tag{9}$$

where the noise components cc and $\hat{v}$ are

$$\begin{aligned} cc(t) &= 1.23 \cdot cc(t-1) - 0.3995 \cdot cc(t-2) + w_{cc}(t) \\ \hat{v}(t) &= 1.013 \cdot \hat{v}(t-1) - 0.2135 \cdot \hat{v}(t-2) + w(t), \end{aligned} \tag{10}$$

with $w_{cc} \sim N(0, 11.3\text{mg}^2/\text{dl}^2)$ and $w \sim N(0, 14.45\ \text{mg}^2/\text{dl}^2)$ (Facchinetti et al., 2014).

We denote the simulation model as Σ_p (cf. Fig. 1). The patient's insulin sensitivity at time t is then given by $S_{I,0} \cdot (1 + Z(t))$, where $S_{I,0}$ is patient-specific, and $(1 + Z(t))$ is the exercise-related increase. The state vector for Σ_p is $(\mathbf{x}, \mathbf{x}_E)$, where $\mathbf{x}_E = (Y, r_{GU}, r_{GP}, Z)$ are the exercise-related states not present in the observer model, while Σ_p lacks an explicit state for the insulin sensitivity.

The parameter values for this simulation model are given in Table A.1. For our simulations, we consider two sources of variation between and within patients: first, we randomly draw the baseline insulin sensitivity $S_{I,0}$ independently for each patient. This means that the UKF has to correctly estimate the initial insulin sensitivity for each patient, as its internal model only uses the average value for $S_{I,0}$, but not the individual value for a patient. Second, the specific carbohydrate content and composition of a meal is usually not known exactly, which can lead to substantial differences in the resulting glucose appearance rate in plasma. To see how the UKF copes with this unknown disturbance, we randomly draw the meal-related parameter m_2 for each patient and each meal independently. Again, the internal model of the UKF only considers the average value of this distribution. The corresponding means and variances are also given in Table A.1.

2.4 Meal and Basal Bolus Calculator

In conventional bolus calculators, the insulin dose is determined from the carbohydrate content of a meal, the deviation of the glucose level from the target and the estimated insulin on board. They are typically of the form

$$u = \frac{CHO}{ICR} + \frac{G - G_t}{CF} - IOB, \tag{11}$$

where u [U] is the insulin bolus, CHO [g] is the amount of carbohydrates, G [mg/dl] is the current glucose concentration and G_t [mg/dl] the target glucose level. Here, we assume that insulin injections are far enough apart such that

the insulin on board, IOB [U], can be neglected. The two parameters ICR [g/U] and CF [mg/dl/U] are the insulin-to-CHO ratio and the correction factor, respectively. Both parameters are patient-specific and related to the individual baseline insulin sensitivity $S_{I,0}$. In clinical practice, both are determined empirically to tailor treatment to an individual patient.

We consider two modifications of the bolus calculator to adjust for the actual insulin sensitivity as estimated by the UKF. To determine a bolus injection for a meal, only the current insulin sensitivity needs to be considered, since changes in insulin sensitivity after exercise are much slower than insulin absorption and meal ingestion. We therefore consider a simple proportional adjustment

$$u_{UKF} = \frac{\hat{S}_{I,0}}{\hat{S}_I} \cdot u, \tag{12}$$

for a bolus insulin dose, where we scale the standard bolus by the ratio of current and baseline insulin sensitivity, estimated as $\hat{S}_I$ and $\hat{S}_{I,0}$ using the UKF (see below). Consequently, an increase in insulin sensitivity would lead to a reduction of the insulin bolus.

With MDI therapy, patients also need to inject long-acting insulin twice a day to achieve a stable basal insulin level. Increased insulin sensitivity can then lead to hypoglcyemia during the night if the evening dose of long-acting insulin is not adjusted. However, the basal insulin level stays roughly constant throughout the night, while insulin sensitivity is slowly decreasing during recovery from exercise. We therefore consider an adjustment of the insulin dose proportional to the average deviation of the insulin sensitivity from the baseline value:

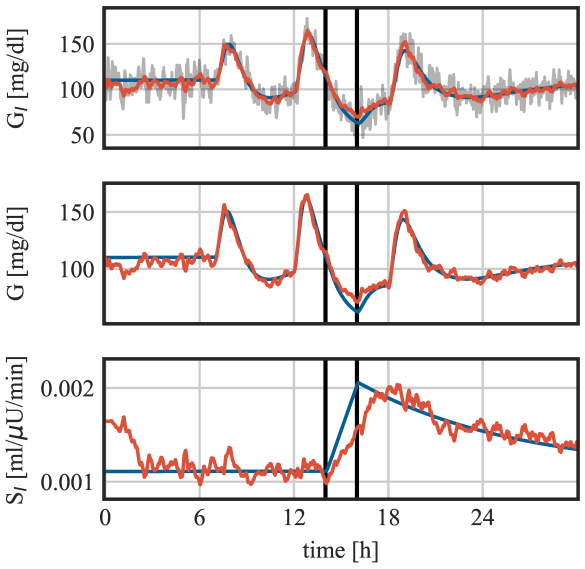

Fig. 2. Estimation of interstitial glucose G_I (top), blood glucose G (center), and insulin sensitivity S_I (bottom), shown for one patient. Simulated noisy observed glucose concentrations from CGM $\tilde{G}_I$ are shown in grey. The true state values are shown as blue lines, their estimates $\hat{G}_I, \hat{G}, \hat{S}_I$ from the UKF in red. Exercise is performed between the two bold vertical lines.

$$u_{b,UKF} = \frac{\hat{S}_{I,0}}{\frac{1}{2}(\hat{S}_I + \hat{S}_{I,0})} \cdot u_b, \tag{13}$$

where u_b [U/min] is the typical basal insulin infusion rate of the patient.

3. RESULTS

We compare the two bolus calculation strategies in a 30h simulation and use the following scenario:

- The UKF is started at 0:00.
- 3 meals are eaten: 60g CHO at 7:00, 80g CHO at 12:00 and 70g CHO at 18:00.
- A correction bolus is computed before each meal using the standard or UKF bolus calculator.
- Moderate intensity exercise is performed at 60% VO_2^{max} (AC=4317 counts/min) from 14:00 to 16:00.
- 15g CHO are ingested after exercise without a meal bolus.
- Basal insulin is adjusted once at 22:00.

For our proof-of-principle, we simulate 25 patients based on the model Σ_p and a basal glucose concentration of $G_b = 110$mg/dl. Since glucose absorption after a meal is highly variable and difficult to capture correctly, we sample an individual meal absorption parameter m_2 for each meal. Moreover, we assign an individual insulin sensitivity $S_{I,0}$ to each patient to capture the high variability in this parameter over patients. In contrast, we use the nominal value for m_2 and the population average value for $S_{I,0}$ for the UKF model Σ_u.

3.1 Tracking of Insulin Sensitivity

First, we test whether we can track insulin sensitivity. Insulin sensitivity increases during exercise and stays elevated for a prolonged period of time. The simulations allow us to assess the ability of the UKF to track these changes, although the underlying changes in physiology are unknown to the observer.

Figure 2 illustrates the estimated interstitial and blood glucose dynamics and estimated insulin sensitivity for one patient. The mismatch between individual and assumed baseline insulin sensitivity is clearly visible at the beginning, and the UKF quickly settles on the patient-specific value ($\hat{S}_{I,0}$). Without an exercise model, the UKF can track the increase in insulin sensitivity during exercise only with a time-lag, but achieves to track the insulin sensitivity and the two glucose states again within a short amount of time after exercise. Then, it follows the slow decrease to the baseline value for the remaining time of the simulation.

3.2 Bolus Calculation

Second, we compare a standard bolus calculator as described in Eq. 11 with our proposed UKF bolus calculators in Eq. 12 and Eq. 13 that adjust for changes in insulin sensitivity. We assume perfect knowledge of the true baseline insulin sensitivity $S_{I,0}$ for each patient for the standard bolus calculator, but we rely on the UKF for estimating this parameter as the average value of $\hat{S}_I(t)$ over the three

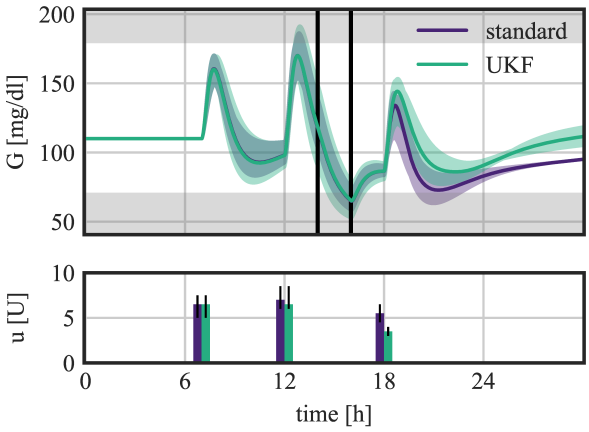

Fig. 3. Blood glucose G (top), and sizes of the meal bolus u (bottom), for the standard (pink) and UKF (green) bolus calculator. Solid lines represent the mean glucose levels, shaded areas show the full range. Exercise was performed between the two bold vertical lines. The three insulin bolus sizes are reported as median and interquartile range.

hours before the first meal for the extended bolus calculator. Our rationale is that the UKF estimate of insulin sensitivity will have settled to the patient-specific baseline over night. We evaluate the performance of each calculator from their resulting blood glucose profiles simulated using the model Σ_p.

Figure 3 shows the glucose levels and the size of the administered correction bolus of all patients for the standard and UKF bolus calculators. Before exercise is started, blood glucose is similar for both approaches and the amount of administered insulin is comparable. This is expected, since insulin sensitivity remains at its baseline level, which does not require any adjustments of the bolus size. Due to noise in the insulin sensitivity estimation, the glucose range of the UKF bolus calculator is slightly wider than the range observed for the standard calculator that profits from perfect knowledge of $S_{I,0}$.

In the evening, insulin sensitivity is elevated after exercise and the bolus administered by the UKF bolus calculator is reduced compared to the standard bolus, leading to higher glucose levels and avoiding excursions into hypoglycemia after dinner. In addition, the basal bolus at 22:00 is reduced to 79.0% [77.0%, 80.3%] of its original size, allowing blood glucose to return to its basal level over night.

Table 1 and 2 summarize the results for both calculators, considering the blood glucose profiles from 6:00 for a full day and from 14:00 when differences between the calculators are expected to arise due to exercise. The time-in-range (TIR) improves under the UKF compared to the standard bolus calculator. The low blood glucose index (LBGI) and high blood glucose index (HBGI) are measures of the extent and number of low, respective high blood glucose events. We observe a reduction in the LBGI and time spent in hypoglycemia (glucose $<$ 70mg/dl) and only a small increase in HBGI for the UKF bolus calculator, indicating less exposure to hypoglycemia without increasing hyperglycemia.

Table 1. Summary of results for the 24h-period starting at 6:00. Numbers are reported as median [interquartile range].

	Standard Calculator	UKF Calculator
TIR (80-140mg/dl) [%]	71.2 [68.5, 73.9]	81.8 [78.2, 82.9]
TIR (70-180mg/dl) [%]	95.6 [93.8, 97.1]	96.9 [95.6, 98.0]
time <70mg/dl [%]	4.4 [2.5, 6.2]	2.8 [1.8, 4.4]
LBGI	2.27 [2.0, 2.42]	1.35 [1.27, 1.46]
HBGI	0.41 [0.36, 0.46]	0.47 [0.41, 0.52]

Table 2. Summary of results from the start of exercise (14:00). Numbers are reported as median [interquartile range].

	Standard Calculator	UKF Calculator
TIR (80-140mg/dl) [%]	69.0 [66.6, 74.8]	85.2 [81.5, 88.4]
TIR (70-180mg/dl) [%]	93.4 [90.6, 96.2]	95.8 [93.4, 97.3]
time <70mg/dl [%]	6.6 [3.8, 9.4]	4.2 [2.7, 6.6]
LBGI	3.16 [2.77, 3.46]	1.8 [1.54, 1.99]
HBGI	0.04 [0.03, 0.05]	0.11 [0.09, 0.15]

4. DISCUSSION

We considered the problem of estimating the increased insulin sensitivity of individual patients following exercise using an unscented Kalman filter. Our observer model comprises previously described model components for insulin administration, meals, and glucose-insulin regulation. However, we deliberately did not include exercise-related changes in this model, presenting a novel approach to track the prolonged rise in insulin sensitivity that does not rely on knowledge of the exercise session and its effects on glucose metabolism. We used the insulin sensitivity estimates from the UKF to propose simple adjustments of the insulin treatment in an extended bolus calculator, where we considered both reduction in bolus insulin for meals following exercise and reduction of basal insulin to prevent hypoglycemia during the night.

We showed that this observer can successfully estimate insulin sensitivity before and after exercise in a 30-hour simulation scenario including unknown patient-specific baseline insulin sensitivity, three meals with unknown, random appearance rates, and a 2-hour exercise session of moderate intensity. Our simulations are based on a patient model that explicitly considers the changes in insulin sensitivity due to exercise. We also showed that considering the actual insulin sensitivity for insulin treatment adjustments can lead to improved glycemic control by increasing the time-in-range and reducing hypoglycemic excursions. This is particularly relevant for calculating meal bolus injections after exercise, and for adjusting the basal insulin rate over night to compensate for increased insulin sensitivity during recovery from exercise.

Our study is a proof-of-principle and thus has several limitations. First, the results are based on in silico simulations, and resulting improvements in glycemic control are conditional on the accuracy of our simulation model. We stress, however, that our observer model does not entail exercise and thus the ability to estimate insulin sensitivity does not depend on the specific patient model for the simulations. Second, we recognize that both simulation and observer model have not been validated on real patient data, even though we emulated existing models for all model components. Third, our results and preliminary fur-

ther studies indicate that explicit consideration of exercise might be required in the observer model to reduce the time-lag between actual and estimated insulin sensitivity during exercise; low glucose sampling rates can aggravate this problem.

Despite these limitations, our study shows that estimating insulin sensitivity before and after exercise is possible from continuous glucose monitoring data, and that considering this estimate when calculating bolus insulin for meals and overnight basal insulin requirements has the potential to reduce exercise-related hypoglycemia.

ACKNOWLEDGEMENTS

We thank Jörg Stelling, Gabor Szinnai, Sara Bachmann, Marie-Anne Burckhardt, Marc Pfister and Eve Tasiudi for discussions.

REFERENCES

American Diabetes Association (2014). Diagnosis and classification of diabetes mellitus. *Diabetes Care*, 37(SUPPL.1), 81–90. doi:10.2337/dc14-S081.

Annan, F. (2016). What matters for calculating insulin bolus dose? *Diabetes Technology and Therapeutics*, 18(4), 213–215. doi:10.1089/dia.2016.0045.

Bergman, R.N., Ider, Y.Z., Bowden, C.R., and Cobelli, C. (1979). Quantitative estimation of insulin sensitivity. *The American journal of physiology*, 236(6), E667–77. doi:10.1172/JCI112886.

Boiroux, D., Aradóttir, T.B., Nørgaard, K., Poulsen, N.K., Madsen, H., and Jørgensen, J.B. (2017). An Adaptive Nonlinear Basal-Bolus Calculator for Patients with Type 1 Diabetes. *Journal of Diabetes Science and Technology*, 11(1), 29–36. doi:10.1177/1932296816666295.

Breton, M.D. (2008). Physical activity-the major unaccounted impediment to closed loop control. *Journal of Diabetes Science and Technology*, 2(1), 169–174. doi:10.1177/193229680800200127.

Cobelli, C., Caumo, A., and Omenetto, M. (1999). Minimal model SG overestimation and SI underestimation: improved accuracy by a Bayesian two-compartment model. *The American journal of physiology*, 277(3 Pt 1), E481–E488.

de Pereda, D., Romero-Vivo, S., Ricarte, B., Rossetti, P., Ampudia-Blasco, F.J., and Bondia, J. (2015). Real-time estimation of plasma insulin concentration from continuous glucose monitor measurements. *Computer Methods in Biomechanics and Biomedical Engineering*, 19(9), 934–942. doi:10.1080/10255842.2015.1077234.

Eberle, C. and Ament, C. (2011). The Unscented Kalman Filter estimates the plasma insulin from glucose measurement. *BioSystems*, 103(1), 67–72. doi:10.1016/j.biosystems.2010.09.012.

Facchinetti, A., Del Favero, S., Sparacino, G., Castle, J.R., Ward, W.K., and Cobelli, C. (2014). Modeling the glucose sensor error. *IEEE Transactions on Biomedical Engineering*, 61(3), 620–629. doi:10.1109/TBME.2013.2284023.

Hovorka, R., Canonico, V., Chassin, L.J., Haueter, U., Massi-Benedetti, M., Federici, M.O., Pieber, T.R., Schaller, H.C., Schaupp, L., Vering, T., and Wilinska, M.E. (2004). Nonlinear model predictive control of glucose concentration in subjects with type 1 diabetes. *Physiological Measurement*, 25(4), 905–920. doi:10.1088/0967-3334/25/4/010.

Janež, A., Guja, C., Mitrakou, A., Lalic, N., Tankova, T., Czupryniak, L., Tabák, A.G., Prazny, M., Martinka, E., and Smircic-Duvnjak, L. (2020). Insulin Therapy in Adults with Type 1 Diabetes Mellitus: a Narrative Review. *Diabetes Therapy*, 11(2), 387–409. doi:10.1007/s13300-019-00743-7.

Julier, S.J. and Uhlmann, J.K. (1997). New extension of the Kalman filter to nonlinear systems. In *SPIE 3068 Signal Processing, Sensor Fusion, and Target Recognition VI*. doi:10.1117/12.280797.

Knobbe, E.J. and Buckingham, B. (2005). The Extended Kalman Filter for Continuous Glucose Monitoring. *Diabetes Technology & Therapeutics*, 7(1), 94–109.

Nucci, G. and Cobelli, C. (2000). Models of subcutaneous insulin kinetics. A critical review. *Computer Methods and Programs in Biomedicine*, 62(3), 249–257. doi:10.1016/S0169-2607(00)00071-7.

Roy, A. and Parker, R.S. (2007). Dynamic Modeling of Exercise Effects on Plasma Glucose and Insulin Levels. *Journal of Diabetes Science and Technology*, 1(3), 338–347. doi:10.3182/20060402-4-BR-2902.00509.

Appendix A. MODEL PARAMETERS

Table A.1. Parameter values for the simulation and observer models. Cells $N(\mu, \sigma^2)$ are parameters drawn from a normal distribution with the indicates mean μ and variance σ^2.

Parameter	Simulation model Σ_p	Observer model Σ_u
p_1	0.008	0.008
p_2	0.015	0.015
p_4	0.058	0.058
p_5	0.0885	0.0885
$S_{I,0}$	$N(1.65 \cdot 10^{-3}, 0.41^2 \cdot 10^{-6})$	$1.65{\cdot}10^{-3}$
EGP_0	3.469	3.469
V_g	1.289	1.289
k_1	0.022	0.022
k_2	0.03	0.03
k_3	0.0021	0.0021
k_4	0.2	0.2
V_i	125	125
m_1	0.0115	0.0115
m_2	$N(0.0513, 0.0128^2)$	0.0513
f	0.93	0.93
τ_G	6.7	6.7
τ_{AC}	5	-
τ_Z	600	-
b	$1.68 \cdot 10^{-6}$	-
q_1	$1.92 \cdot 10^{-7}$	-
q_2	0.078	-
q_3	$1.19 \cdot 10^{-7}$	-
q_4	0.048	-
a	1500	-
n	20	-